

Muh Sarkowi

Microtremor Analysis to Evaluate BMKG Region III Building, Bali, Ind...

Sources Overview

8%

OVERALL SIMILARITY

1	link.springer.com INTERNET	<1%
2	www.sciencegate.app INTERNET	<1%
3	Juan Pandu Gya Nur Rochman, Amien Widodo, Dwa Desa Warnana, Wien Lestari, Mariyanto, Nita Ariyanti, Jeremy Reviel Karo Karo. "Microzonatio... CROSSREF	<1%
4	www.nat-hazards-earth-syst-sci.net INTERNET	<1%
5	repository.lppm.unila.ac.id INTERNET	<1%
6	tel.archives-ouvertes.fr INTERNET	<1%
7	G Yuliyanto, M I Nurwidyanto. "Analysis of landslide in Bungkah, Sepakung, Banyubiru using ground shear strain method and shear wave profile fr... CROSSREF	<1%
8	Mayada Al-kousa, Hala Tawfiq Hasan, Mohamad khir Abdul-wahed, Maissa Alarab, Idmon Al-egy. "Experimental and analytical evaluation of the c... CROSSREF	<1%
9	Universitas Sebelas Maret on 2019-08-28 SUBMITTED WORKS	<1%
10	University of Liverpool on 2018-05-04 SUBMITTED WORKS	<1%
11	School of Business and Management ITB on 2019-05-20 SUBMITTED WORKS	<1%
12	jurnal.uns.ac.id INTERNET	<1%
13	www.asian-transactions.org INTERNET	<1%
14	ocs.unud.ac.id INTERNET	<1%
15	Universitas Brawijaya on 2019-08-01 SUBMITTED WORKS	<1%
16	D Widyawarman. "Subsurface Identification of Campus I Universitas PGRI Yogyakarta using The Microtremor Wave Method", Journal of Physics: ... CROSSREF	<1%
17	NAF Tanjung, I Permatasari, AHP Yuniarto. "Mapping of weathered layer thickness and Seismic Vulnerability in Tegal using HVSR method", Journ... CROSSREF	<1%
18	Pan, Tso-Chien, Key Seng Goh, and Kusnowidjaja Megawati. "Empirical relationships between natural vibration period and height of buildings in Si... CROSSREF	<1%

19	Syiah Kuala University on 2019-04-12 SUBMITTED WORKS	<1%
20	Universitas Brawijaya on 2019-07-31 SUBMITTED WORKS	<1%
21	archive.org INTERNET	<1%
22	www.geologija-revija.si INTERNET	<1%
23	www.tandfonline.com INTERNET	<1%
24	Dipendra Gautam. "Ambient Vibration Measurements in Representative Buildings in Kathmandu Valley Following the Gorkha Earthquake", Journal ... CROSSREF	<1%
25	NATO Science for Peace and Security Series C Environmental Security, 2009. CROSSREF	<1%
26	Instanbul bilgi Universitesi - Psychology on 2009-06-01 SUBMITTED WORKS	<1%
27	International Institute of Information Technology, Hyderabad on 2021-07-28 SUBMITTED WORKS	<1%

Excluded search repositories:

None

Excluded from document:

Bibliography
Citations

Excluded sources:

None

1 **Microtremor Analysis to Evaluate BMKG Region III Building, Bali,** 2 **Indonesia**

3 4 **Abstract**

5 Bali Island has experienced more than 6 significant earthquakes (magnitude > 6) since
6 1815, which caused extensive damage to buildings and casualties. The microtremor data
7 analysis in the building of Indonesian¹⁴ meteorology, climatology and geophysics agency
8 (BMKG) Region III Denpasar aims to reduce the risk of building damage and casualties due to
9 the earthquake. The analysis was conducted by measuring microtremor and processing the data
10 to obtain the natural frequency of the soil (f_{0s} HVSR) and building (f_{0b} HVSR), resonance, soil
11 (Kg), and building vulnerability index (Kb) so that the safety of the building can be known in
12 the event of an earthquake. The processing and analyzing results the characteristics of
13 microtremor data get the f_{0b} has a greater value than the f_{0s} value so that the building is relatively
14 safe from resonance. The resonance value of the building with the ground has an (R) value of
15 6.67% - 13.3%, with an average resonance value of 8.89% which is included in the medium
16 resonance. The location of the building is in an area with a Kg of 8.20 – 10.81, which is included
17 in the category of low to moderate soil vulnerability index, and the Kb has a value of 0.4827×10^{-6}
18 $- 7.9771 \times 10^{-6}$, with the first floor having an index highest vulnerability. The f_{0s} , f_{0b} , R , Kg ,
19 and Kb show that the building is in the safe category in the event of an earthquake.

20
21 **Keywords:** Microtremor, natural frequency, resonance, vulnerability building, Bali

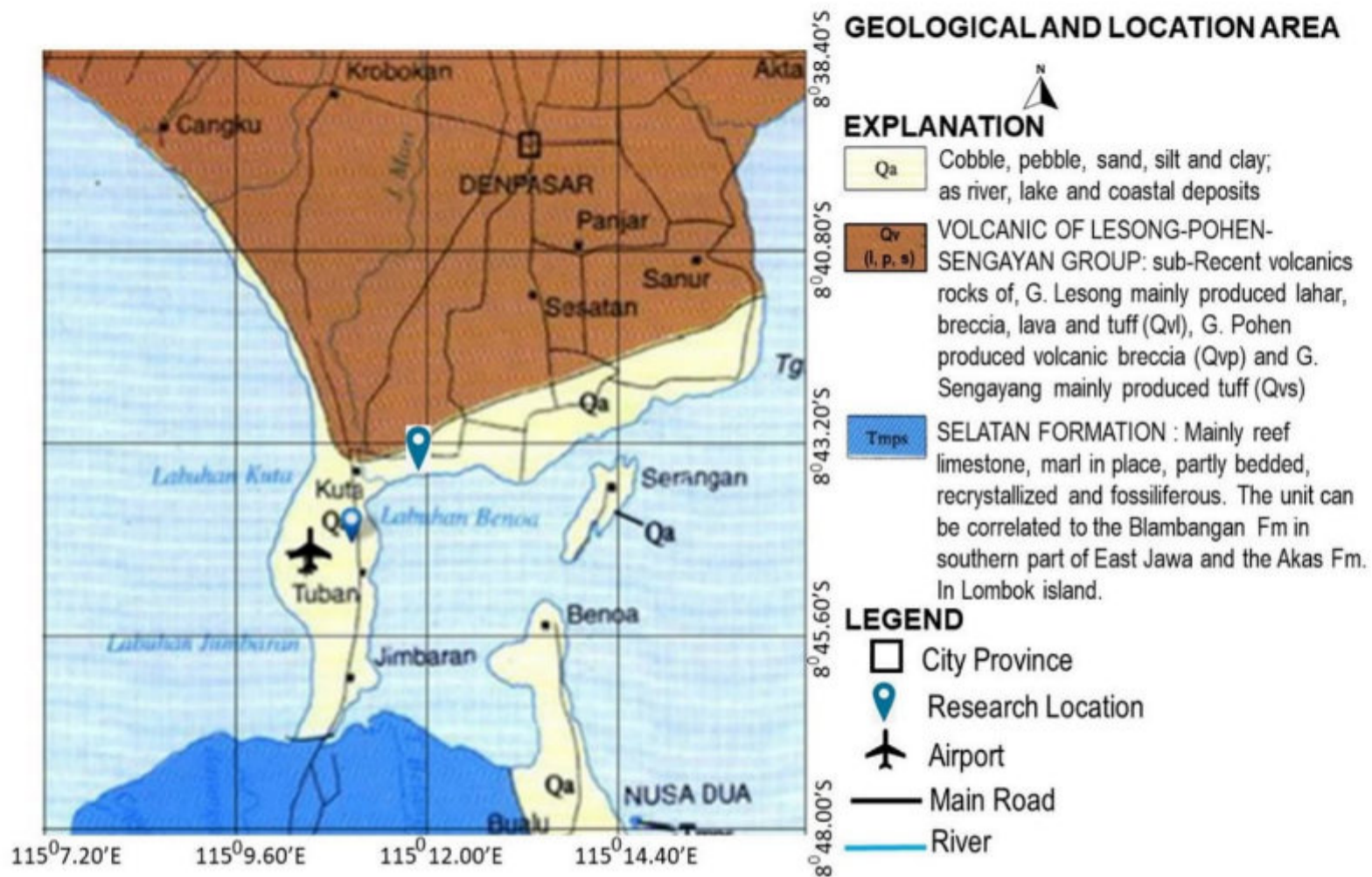
22

23 **1. Introduction**

24 Bali, which is located in a subduction zone between the Indo-Australian Plate and the
25 Eurasian plate, and the presence of Back Arc Thrust tectonic activity in the north, causes a high
26 potential for earthquakes (Daryono 2011). Historical records show that some large earthquakes
27 with a magnitude > 6 on the Richter Scale caused massive loss of life and damage in 1815,
28 1857, 1917, 1976, 2011, and 2019 (Maharani 2020).

29 Earthquakes cause shaking and shaking of the building structure, which can cause damage
30 to the building. Therefore, designing a building is necessary to consider the factors that can
31 damage the structure of the building due to an earthquake. A safe and earthquake-resistant
32 building is a building that meets SNI 1726:2002 (BSN 2002) concerning procedures for
33 planning earthquake resistance. In addition, the building also has a natural frequency that is
34 greater than the ²⁷natural frequency of the soil. The value of the resonance index and the value
35 of the vulnerability of the building is small (Gosar 2007). The natural frequency value can be
36 influenced by its size, shape, and composition (Nakamura 2000).

37 The BMKG Region III building is located in Kuta city, Bali. That building geologically
38 in the Quaternary alluvium Formation with gravel to gravel sand texture, silt, and clay which
39 is the product of the river, lake, and beach deposits (Fig 1) (Hadiwidjojo et al. 1998). The
40 location of the BMKG Region III Bali building has a small amplification and dominant
41 frequency, with a large seismic vulnerability index and a significant ground shear strain value
42 so that the research location has a high potential for damage (Kurniawan et al. 2017). However,
43 research has not been conducted on building resonance and building vulnerability index,
44 especially the BMKG Region III Denpasar building.



45

46 Fig 1. Geological map and location of the research area (modified from Hadiwidjojo et al.
47 (1998)).

48

49 From a geological point of view, if an earthquake occurs, the BMKG Region III building
50 in Bali is in an area with a high potential for damage. So that in this study, measurements and
51 processing of microtremor data will be carried out to obtain building safety values. The natural
52 frequency value on the soil is carried out by processing microtremor data using the horizontal
53 to vertical spectral ratio method (Konno & Ohmachi 1998; Gallipoli et al. 2004; Över et al.
54 2011; Abdialim et al. 2021)). Whereas the natural frequency value in the building is determined
55 using the floor spectral ratio method and the analysis spectrum results from each floor to the
56 ground below it to get the natural frequency building value (Gosar 2007; Triwulan et al. 2010;
57 Prakosa et al. 2015).

58

59 The results obtained from processing the two methods are natural frequency values, but
60 resonance and amplification values will be obtained. The building resonance value is
determined based on the spectrum for each component (NS and EW). Resonance can be used

61 to determine the level of possibility of a building experiencing resonance during an earthquake
62 (Gosar et al. 2010).

63 The value of the amplification and natural frequency in soil and buildings can be used for
64 further analysis to obtain the value of soil vulnerability analysis (Büyüksaraç et al. 2013; Bekler
65 et al. 2019), building vulnerability analysis, and building resonance. The level of building
66 damage is directly proportional to the soil vulnerability index (Nakamura 2000).

67

68 2. Theory

69 2.1. Microtremor

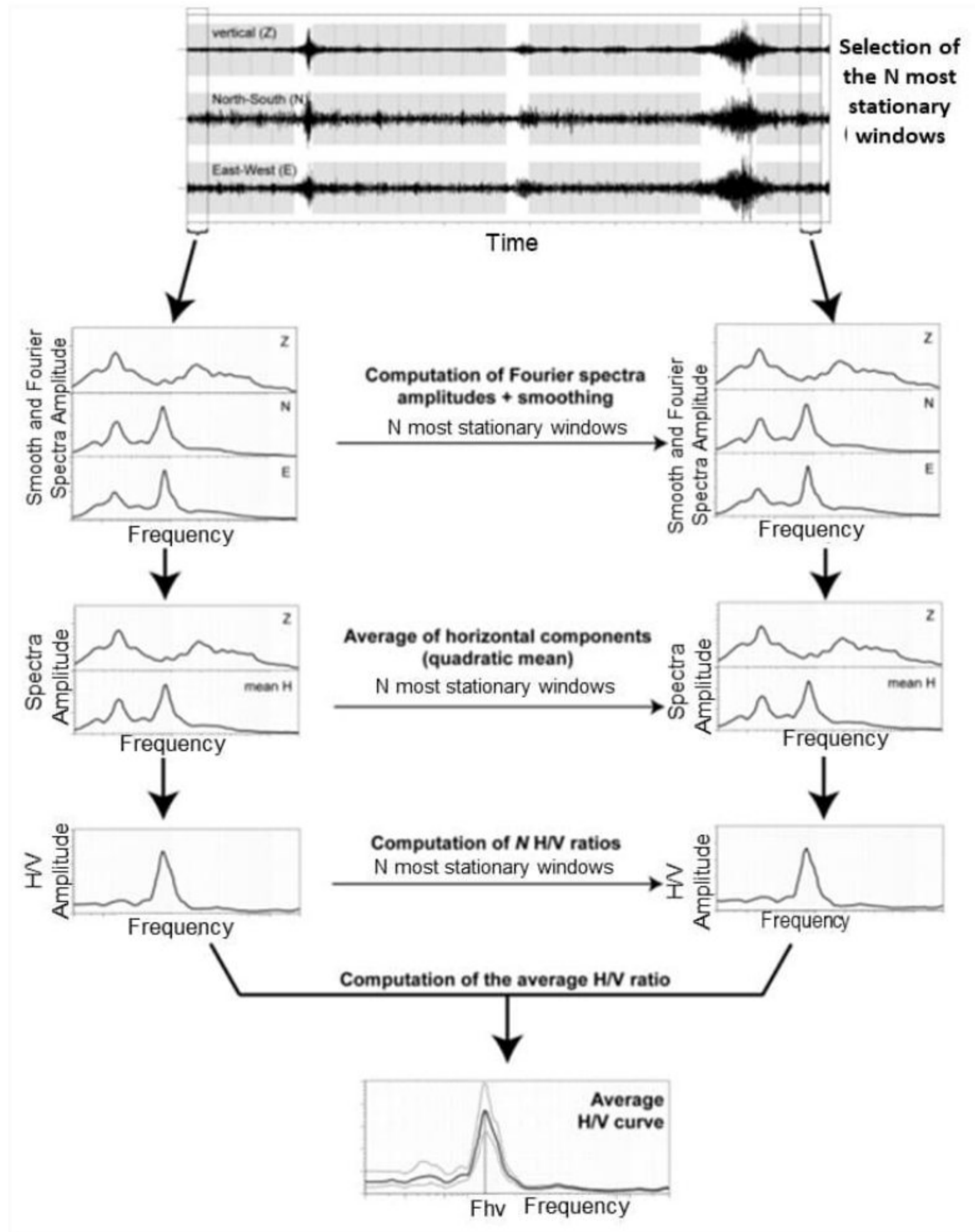
70 Microtremor is a ground vibration that human activities or natural activities can cause.
 71 Microtremor can occur due to vibrations caused by walking, car vibrations, engine vibrations,
 72 wind vibrations, ocean waves, or natural vibrations from the ground (Tokimatsu 1995).
 73 Microtremor has a higher frequency than the frequency of earthquakes, and the ⁹period is less
 74 than 0.1 seconds which is generally between 0.05 - 2 seconds. It can be 5 seconds for long
 75 period microtremors, while the amplitude ranges from 0.1 to 2.0 microns. Microtremor is a
 76 ground vibration that propagates in the form of waves called microseismic waves. Recently,
 77 microtremor applications have been used to identify the natural resonance frequencies of
 78 buildings and soils (Gallipoli et al. 2004; Gosar 2007; Gosar et al. 2010).

79 Microtremor can be used to design earthquake-resistant buildings by knowing ²⁴the natural
 80 period of the local soil to avoid resonance. The measured microtremor data consists of 3
 81 components, namely: ²vertical (up and down), horizontal (N-S), and horizontal (E-W). After
 82 obtaining the signal, it can then be analyzed using the HVSR method and obtain the dominant
 83 frequency and amplification values. This HVSR method compares the spectrum ratio of the
 84 horizontal component of the microtremor signal to its vertical component (Nakamura 1989).

85 The HVSR analysis method developed by Nakamura (1989) calculates the ratio of the
 86 Fourier spectrum of the horizontal component of the microtremor signal to its vertical
 87 component. The HVSR processing process, in general, can be seen in Fig 2. Mathematically
 88 Horizontal to vertical spectra ratio is expressed in equation 1 (Nakamura 1989).

$$89 \quad R(f) = \frac{\sqrt{H_{EW}^2(f) + H_{NS}^2(f)}}{V_{UD}(f)} \quad (1)$$

90 Where $R(f)$ is the spectrum of the HVSR ratio, $H_{EW}(f)$ ²⁵ is the spectrum of the horizontal
 91 component E-W, $H_{NS}(f)$ ¹⁰ is the spectrum of the horizontal N-S component and $V_{UD}(f)$ is the
 92 spectrum of the vertical component.



93

94 Fig 2. The flowchart shows the computation steps of the H/V ratio (Fergany & Omar 2017).

95 The results of the HVSR analysis showed a spectrum peak at the dominant frequency. The
 96 dominant frequency (f_0) and the amplification factor (A) that describe the dynamic
 97 characteristics of the soil can be generated from the HVSR analysis (Nakamura 2000).
 98 Microtremor is mainly used to identify the soil's dominant frequency, the building's dominant
 99 frequency, and the resonance frequency of the building and soil structure beneath it (Moon et
 100 al. 2019).

101 The floor spectra ratio (FSR) method is a method for determining the natural and resonant
 102 frequencies of buildings that describe the characteristics of buildings against earthquakes
 103 (Gosar et al. 2010). In the FSR method, other building characteristics that can be obtained
 104 besides the natural frequency are the building resonance index and the building vulnerability
 105 index. The natural frequency building value is determined from the spectrum analysis of each
 106 building floor to the ground below it. The data calculation process is carried out to determine
 107 the natural frequency value of the building using equations (2) and (3) (Prakosa et al. 2015).

$$108 \quad f_0(FSR) = \frac{f_b^{NS}}{f_t^{NS}} \quad (2)$$

$$109 \quad f_0(FSR) = \frac{f_b^{EW}}{f_t^{EW}} \quad (3)$$

110 Equations (2) and (3) are FSR analysis equations where f_b is the value of the building
 111 frequency, f_t is the value of the ground frequency, and NS-EW is the respective components of
 112 the data.

113 Resonance can be used to determine the level of possibility of a building experiencing
 114 resonance during an earthquake (Gosar et al. 2010). There are several classifications:

- 115 1. Low resonance ($R > 25\%$)
- 116 2. Medium resonance ($15\% < R < 25\%$)

117 3. High resonance ($R < 15\%$)

118 The building resonance index (R) is determined based on the spectrum of each component
 119 (NS and EW) which is calculated based on the following equation:

$$120 \quad R = \left| \frac{f_b - f_t}{f_t} \right| \times 100\% \quad (4)$$

121 Where f_b is the natural frequency of the building, and f_t is the natural frequency of the
 122 ground.

123 The level of building damage is directly proportional to the soil vulnerability index (Kg).
 124 Soil vulnerability index is the vulnerability of the soil surface that results in deformation during
 125 earthquake waves. This vulnerability can be associated with lateral ground motion due to weak
 126 zones and fluid-filled rock pores.

127 Mathematically the formula for soil vulnerability index can be formulated in equation (5)
 128 (Nakamura 2000; Sungkono et al. 2011).

$$129 \quad Kg = \frac{Am^2}{f_0} \quad (5)$$

130 where Kg is the soil susceptibility index, Am is the peak of the HVSR spectrum, and f_0 is
 131 the dominant frequency value. The value of the soil vulnerability index is classified to
 132 determine the level of vulnerability that can occur due to earthquakes.

133 Table 2.1 Classification of soil vulnerability index values (Wulandari et al. 2018; Nakamura
 134 1997).

Zone	Kg value
Low	<3
Medium	3-6
High	>6

135

136 2.2. Building Vulnerability Index

137 The building vulnerability index can be estimated from the structure deformation
138 associated with the seismic movement in the ground and the ²⁶dynamic characteristics of the
139 surface layers and structures. This is to estimate the possibility of damage to the building in an
140 earthquake in the future, for example, to calculate the vulnerability index of buildings using
141 equations (Mucciarelli et al. 2007; Sungkono et al. 2011; Sato et al. 2008; Akkaya 2020;
142 Lantada et al. 2009):

$$143 \quad K_{bi} = \frac{A}{4\pi^2 f_0^2 \cdot h_i} \quad (6)$$

144 Where A is the amplification factor of the FSR analysis on the soil and structure of the i -
145 th floor. f_0 is the frequency value of the building's spectrum, and h_i is the height of the building
146 on the i -th floor.

147

148

149 **3. ²¹Methods**

150 The research data used in this study are borehole accelerometer data located at a depth of
151 8 meters from the ground surface and accelerometer data located on the 1st, 2nd, and 3rd floors
152 of the BMKG Building Region III Denpasar – Bali (Fig 3). The accelerometer used is the
153 Raspberry Shake 4D Strong Motion Seismograph which measures three-wave components
154 (east-west, north-south, and vertical components). Accelerograph data on boreholes were taken
155 on July 31, 2020, and October 2, 2020, while accelerometer data on the 1st, 2nd, and 3rd floors
156 were measured on September 24, 2020, from 03:00 to 13:00 eastern Indonesia time region (Fig
157 4).

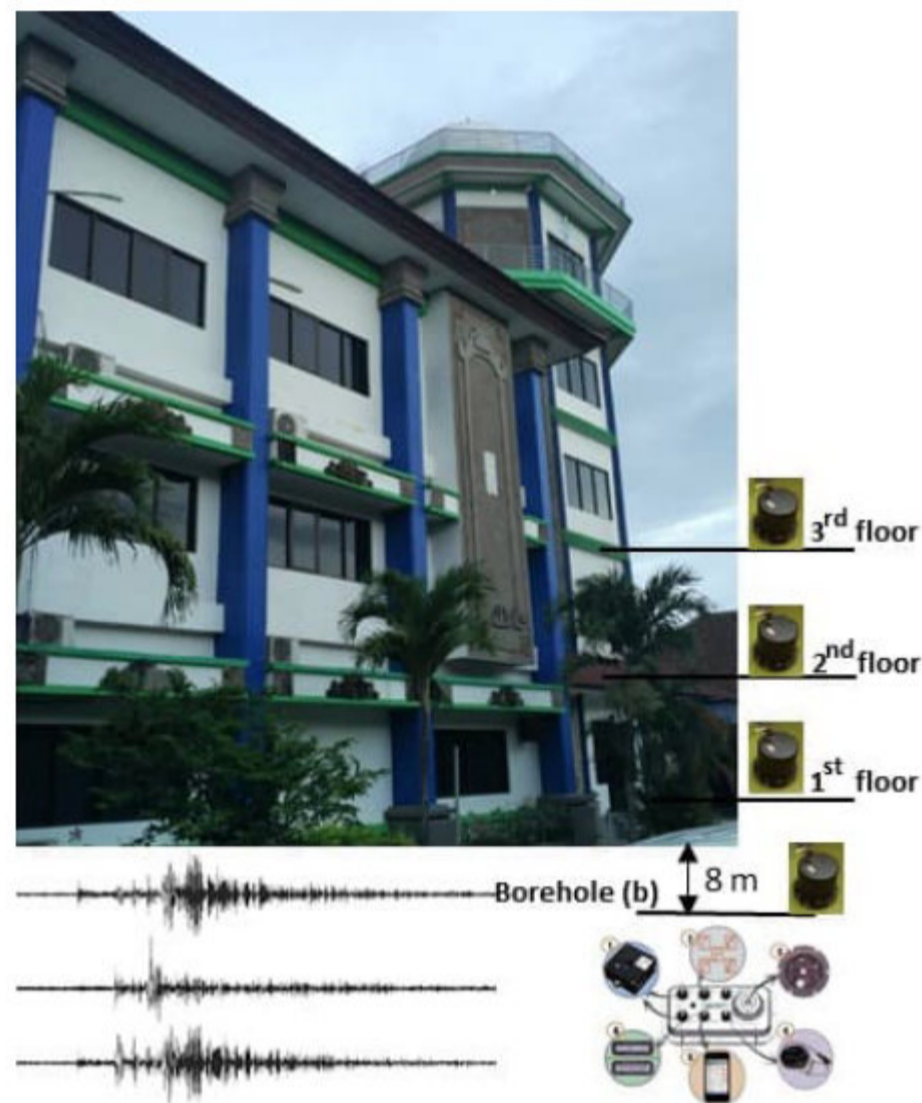
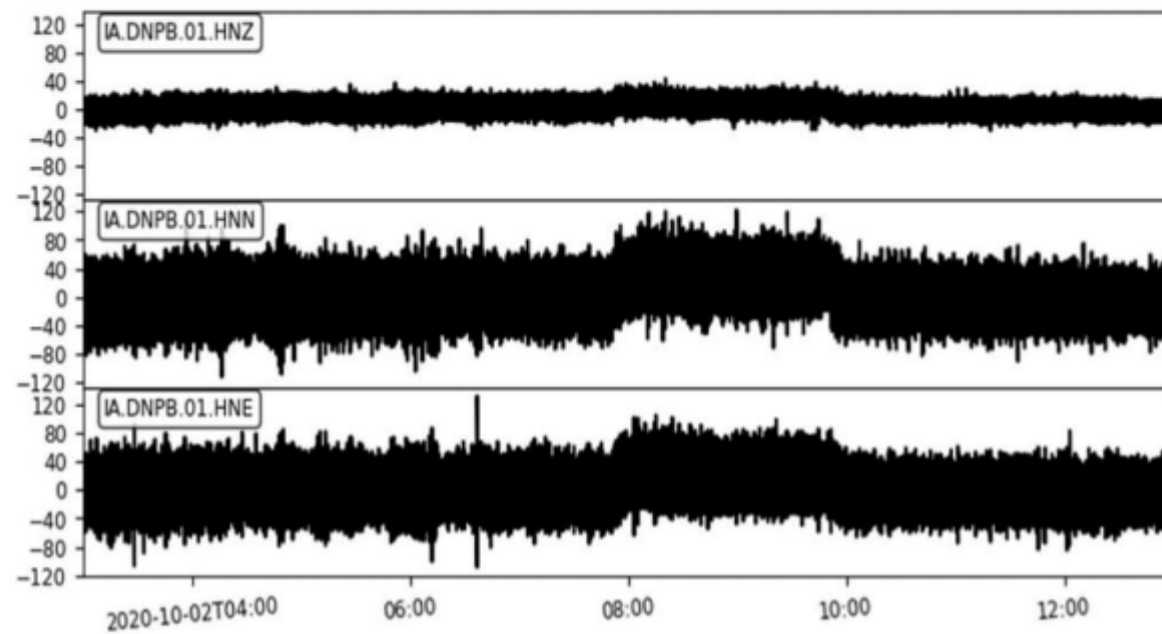


Fig 3. Location of the borehole accelerometer and building accelerometer.



160

161 Fig 4. Accelerometer data were recorded at the borehole on October 2, 2020, from 03:00 to
162 13:00.

163 Processing of HVSR and FSR is carried out to obtain the value of the natural frequency²³
164 of the soil, the natural frequency of the building,⁷ and the amplification factor. To find out the
165 condition of the vulnerability of the building due to vibration, natural frequency analysis of the
166 soil is carried out, natural frequency analysis of buildings, building resonance analysis, soil
167 vulnerability index analysis, and building vulnerability index analysis is carried out.

168

169 **4. Result discussions**

170 4.1. Ground Natural Frequency

171 The results of processing soil microtremor data (boreholes) consisting of: natural
 172 frequency of the soil E – W direction (f_{0s} E-W), the amplitude of the soil E – W direction (A_{0s}
 173 E-W), the natural frequency of the soil N – S direction (f_{0s} N-S), the amplitude of the soil N –
 174 S direction (A_{0s} N-S), the natural frequency of the soil U-D direction (f_{0s} U-D), the amplitude
 175 of the soil U–D direction (A_{0s} U-D), horizontal to a vertical ratio (HVSR) on July 31, 2020,
 176 and October 2, 2020 data are shown at Table 1, Table 2, Fig. 5, and Fig. 6, respectively.

177 Table 1. The ¹ natural frequency of the soil value, horizontal to vertical spectrum ratio, and
 178 amplitude at July 31, 2020.

f_{0s} E-W (Hz)	A_{0s} E-W	f_{0s} N-S (Hz)	A_{0s} N-S	f_{0s} U-D (Hz)	A_{0s} U-D	f_{0s} HVSR (Hz)	A_{0s} HVSR
0.15	0.79	0.15	0.32	0.15	0.32	0.32	1.86

179

180 Table 2. The ¹ natural frequency of the soil value, horizontal to vertical spectrum ratio, and
 181 amplitude at October 2, 2020.

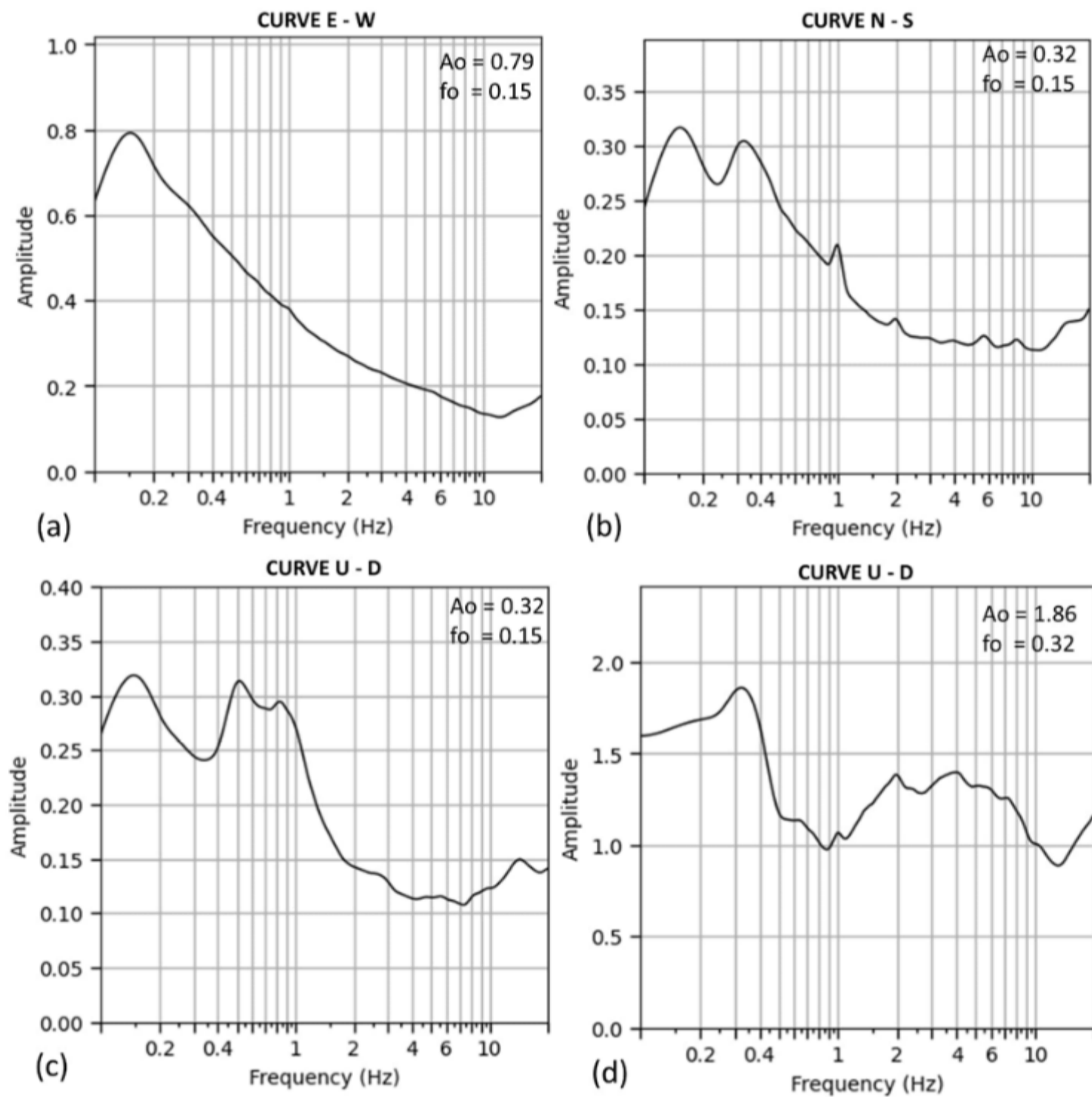
f_{0s} E-W (Hz)	A_{0s} E-W	f_{0s} N-S (Hz)	A_{0s} N-S	f_{0s} U-D (Hz)	A_{0s} U-D	f_{0s} HVSR (Hz)	A_{0s} HVSR
0.15	0.55	0.15	0.29	0.52	0.29	0.32	1.62

182

183 According to Kanai (1983), the value of the natural frequency of this soil is included in
 184 the soil classification type-I (f_{0s} soil < 2.5 Hz) with a fairly thick sediment thickness, alluvial
 185 rock formed from delta sedimentation, topsoil, mud, and others with a depth of 30m or more.
 186 These results follow the study area's geological data, which consists of the Quaternary
 187 Alluvium Formation or the Holocene era, which has a lithology of gravel, gravel, sand, silt,
 188 and clay from the river, lake, and beach deposits (Hadiwidjojo et al. 1998).

189 Among the causes of ²² variations in the shape of the HVSR curve are variations in

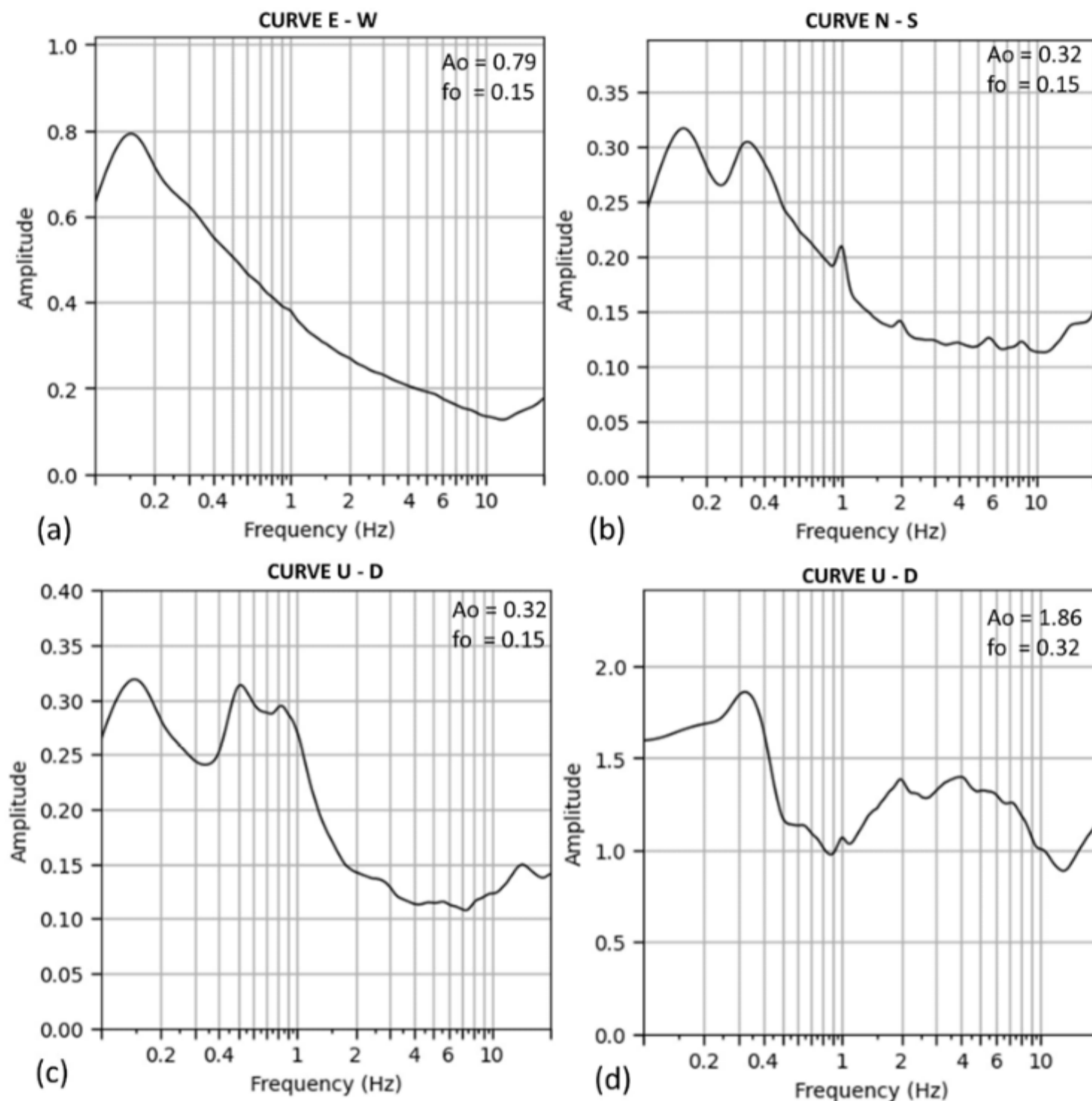
190 impedance contrast, layer compactness, rock hardness, subsurface geology, and others. Herak
 191 (2008) mentions six parameters that affect the HVSR curve, namely primary wave velocity
 192 (V_p), shear wave velocity (V_s), layer thickness (h), layer density (ρ), quasi wave factor (Q_p
 193 and Q_s).



194

195 Fig 5. The results of processing the ⁴ fast Fourier transform microtremor data to obtain the natural
 196 frequency value of the waves and the HVSR curve ⁸ to obtain the natural frequency of the soil
 197 for the data on July 31, 2020. (a) The natural frequency curve of the E-W component
 198 microtremor wave; (b) The natural frequency curve of the N-S component microtremor wave;
 199 (c) The natural frequency curve of the Z (U-D) component microtremor wave; (d) The HVSR

200 curve of the soil (f_0 HVSR)



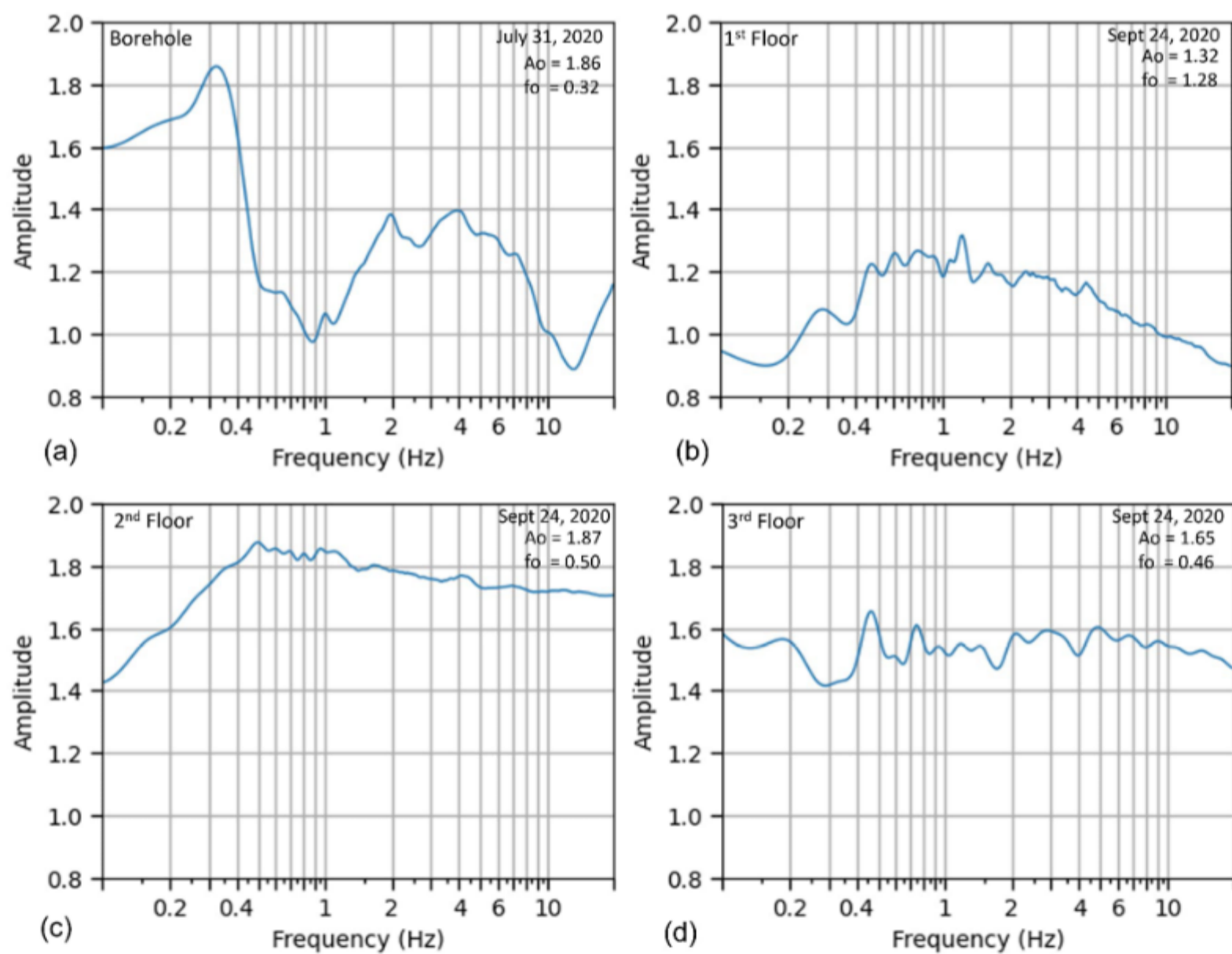
201

202

203 Fig 6. The results of processing the ⁴ fast Fourier transform microtremor data to obtain the natural
 204 frequency value of the waves and the HVSR curve ⁸ to obtain the natural frequency of the soil
 205 for the data on July 31, 2020. (a) The natural frequency curve of the E-W component
 206 microtremor wave; (b) The natural frequency curve of the N-S component microtremor wave;
 207 (c) The natural frequency curve of the Z (U-D) component microtremor wave; and (d) The
 208 HVSR curve of the soil (f_0 HVSR).

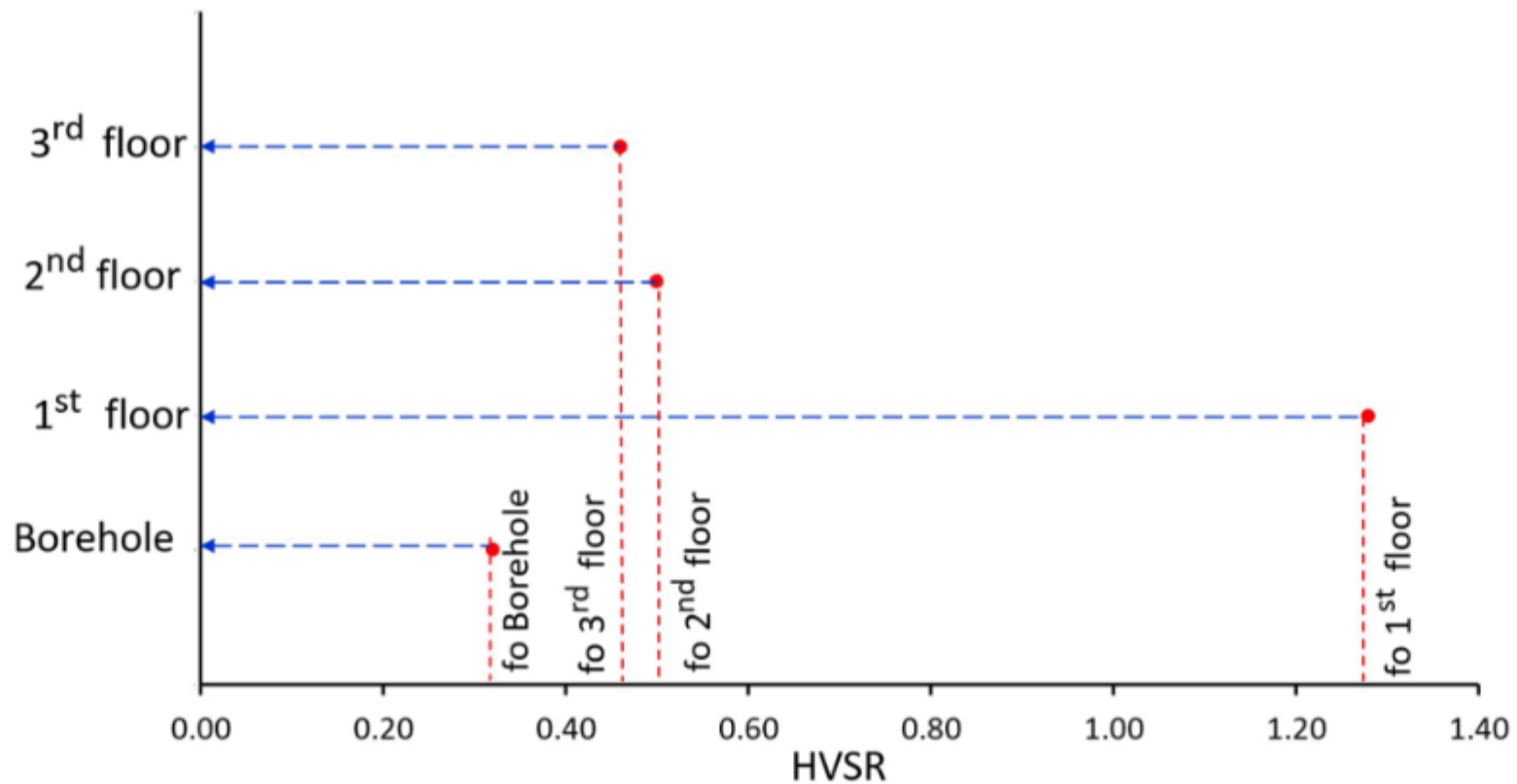
209 4.2. Building Natural Frequency

210 Microtremor data processing has been carried out on the 1st, 2nd, and 3rd floors measured
 211 on September 24, 2020, from 03:00 to 13:00 eastern Indonesia time region (Fig 7) to get the
 212 natural frequency value. The results of the calculation of the dominant frequency of the
 213 building (f_{ob}) using the equation given by Nakamura (1989) get the value of the dominant
 214 frequency of the building (f_{ob}) on the 1st floor = 1.28 Hz, the value of the dominant frequency
 215 of the building (f_{ob}) on the 2nd floor = 0.5 Hz, and the dominant frequency value of the building
 216 (f_{ob}) on the 3rd floor = 0.46 Hz (Fig 8). The calculation results show that the value of the
 217 building's dominant frequency (f_{ob}) has the best value compared to the height of the building.
 218 The higher the building the value will have, the smaller the building's dominant frequency (f_{ob}).
 219 The value of the natural frequency of the building (f_{ob}) BMKG Region III has a greater value
 220 than the value of the dominant ground frequency (f_{ot}) so that the building is relatively safe from
 221 resonance.



222

223 Fig 7. The horizontal to vertical spectral ratio curve of microtremor data processing results on
 224 the 1st, 2nd, and 3rd floors were measured on September 24, 2020, from 03:00 to 13:00 eastern
 225 Indonesia time region.



226

227 Fig 8. Graph of the relationship between the location of the microtremor measurement in the
 228 BMKG Region III Denpasar building with f_0 HVSr value.

229 4.3. Resonance Building and Ground (R)

230 The resonance value of the building with the ground has a value of 6.67% - 13.3%, with
 231 an average resonance value of 8.89%. Based on the classification made by Gosar et al. (2010),
 232 the resonance value obtained is included in the high resonance because the natural frequency
 233 of the building value is close to or equal to the value of the natural frequency of the soil. The
 234 resonance percentage value between the building and the ground is strongly influenced by the
 235 difference in value between the soil's natural frequency and the natural frequency of the
 236 building above it. For example, suppose the natural frequency of the building is closer to the
 237 natural frequency of the soil. In that case, the resonance percentage value is getting smaller,
 238 which means that the building vulnerability level to the soil is getting higher, and the resonance

239 possibility between the soil and the building is also getting more significant. On the other hand,
 240 if the natural frequency value of the land and the buildings has a more significant difference,
 241 then the value of the resonance percentage is more significant, meaning that the level of
 242 vulnerability of the building to the soil is low. The possibility of resonance between the soil
 243 and the building is also getting smaller.

244 4.4. Soil Vulnerability Index

245 The results of processing soil vulnerability using the equation that Nakamura (2000) and
 246 Sungkono et al. (2011) get a soil vulnerability value of 10.81 for the measurement results on
 247 July 31, 2020, and 8.20 for the measurement on October 2, 2020. The results of the soil
 248 vulnerability index are following the results research conducted by previous researchers found
 249 that the research area was included in the category of low to moderate vulnerability index,
 250 namely $0.95 < K_g < 18.76$ (Murdiantoro et al. 2016; Kurniawan et al. 2017; Pratama et al. 2020).
 251 According to Daryono et al. (2009), $K_g < 10$ has a low soil vulnerability index, $10 < K_g < 20$ is in
 252 the medium category, and $K_g > 20$ is classified in the hazard zone.

253 4.5. Building Vulnerability Index

254 The building vulnerability index (K_b) shows the level of damage that occurs to the
 255 building in the event of an earthquake. The greater the vulnerability value of a building, the
 256 greater the potential damage that will occur (Sato et al. 2008). The data processing results get
 257 the vulnerability index value (K_b) of the BMKG building between 0.4827 to 7.9771. The 1st
 258 floor has the high vulnerability index, and the 3rd floor has the lowest vulnerability index (Table
 259 3).

260 Table 3. Building Vulnerability Index Table.

Location	Building Vulnerability	Building Vulnerability
----------	------------------------	------------------------

	Index (<i>Kb</i> E-W)	Index (<i>Kb</i> N-S)
1 st Floor	0.931015	7.977052
2 nd Floor	0.590797	5.213707
3 rd Floor	0.482705	0.812579

261

262

263

264 **5. Conclusions**

265 The results of processing and analyzing the characteristics of microtremor data in the
266 BMKG Region III Denpasar Bali building get:

- 267 1. The natural frequency value of soil (f_{os}) 0.28 Hz - 0.29 Hz, which is included in the
268 soil classification type I (f_{os}) soil < 2.5 Hz) with a fairly thick sediment thickness,
269 ³alluvial rock formed from delta sedimentation, topsoil, and mud. with a depth of 30 m
270 or more. These are consistent with the geology, which consists of the Quaternary
271 alluvium Formation, which has a lithology of gravel-to-gravel sand, silt, and clay from
272 the river, lake, and beach deposits.
- 273 2. The dominant frequency value of the building (f_{ob}) on each building is 1.28 Hz on the
274 1st floor, 0.5 Hz on the 2nd floor, and 0.46 Hz on the 3rd floor. The natural frequency of
275 the building (f_{ob}) value has a greater value than the dominant ground frequency (f_{ot})
276 so that the building is relatively safe from resonance.
- 277 3. The building's resonance value (R) with the ground is 6.67% - 13.3%, with an average
278 resonance value of 8.89%, and that value is the high resonance category; because the
279 natural frequency value ¹⁵of the building is not close or equal to the natural frequency
280 value of the soil.
- 281 4. The building is located in an area with a soil vulnerability (K_g) value of 8.20 – 10.81,
282 which is included in the low to moderate soil vulnerability index. Meanwhile, the
283 building vulnerability index (K_b) found that the building has a value of 0.4827 –
284 7.9770, with the 1st floor having the highest vulnerability index. The ³value of the
285 building vulnerability index shows that it is in a low category (safe).

286

287

288

289

290

291

292

293

294 **Acknowledgments**

295 The authors appreciate the financial support from the Research institute and community
296 engagement Universitas Lampung and Engineering Faculty Universitas Lampung.

297

298 **References**

- 299 Akkaya İ (2020) Availability of seismic vulnerability index (Kg) in the assessment of building
300 damage in Van, Eastern Turkey. *Earthquake Engineering and Engineering Vibration*,
301 *19*(1), 189–204. [https://doi.org/https://doi.org/10.1007/s11803-020-0556-z](https://doi.org/10.1007/s11803-020-0556-z).
- 302 Abdialim S, Hakimov F, Kim J, Ku T, and Moon SW (2021) Seismic site classification from
303 HVSR data using the Rayleigh wave ellipticity inversion: a case study in Singapore.
304 *Earthquakes and Structures*, *21*(3). doi.org/10.12989/eas.2021.21.3.231.
- 305 Badan Standarisasi Nasional (2002) Standar Perencanaan Ketahanan Gempa untuk Struktur
306 Bangunan Gedung (SNI 1726-2002).
- 307 Bekler T, Demirci A, Ekinci YL, Büyüksaraç A (2019) Analysis of local site conditions through
308 geophysical parameters at a city under earthquake threat: Çanakkale, NW Turkey.
309 *Journal of Applied Geophysics*, *163*, 31-39.
- 310 Büyüksaraç A, Bektaş Ö, Yılmaz H, Arısoy MÖ (2013) Preliminary seismic microzonation of
311 Sivas city (Turkey) using microtremor and refraction microtremor (ReMi) measurements.
312 *Journal of Seismology*, *17*(2), 425–435.
- 313 Daryono, Sutikno, Sartohadi J, Dulbahri, & Brotopuspito KS (2009) Efek tapak lokal di Graben
314 bantul berdasarkan pengukuran mikrotremor. *International Conference Earth Science and*
315 *Technology*.
- 316 Daryono (2011) Identifikasi Sesar Naik Belakang Busur (*Back Arc Thrust*) Daerah Bali
317 Berdasarkan Seismisitas dan Solusi Bidang Sesar. *Artikel Kebumihan, Badan Meteorologi*
318 *Klimatologi dan Geofisika*.
- 319 Fergany E, & Omar K (2017) Liquefaction potential of Nile delta, Egypt. *NRIAG Journal of*
320 *Astronomy and Geophysics*, *6*(1), 60–67. <https://doi.org/10.1016/j.nrjag.2017.01.004>.
- 321 Gallipoli MR, Mucciarelli M, Castro RR, Monachesi G, & Contri P (2004) Structure, soil-

- 322 structure response and effects of damage based on observations of horizontal-to-vertical
323 spectral ratios of microtremors. *Soil Dynamics and Earthquake Engineering*, 24(6), 487–
324 495. <https://doi.org/10.1016/j.soildyn.2003.11.009>.
- 325 Gosar A (2007) Microtremor HVSR study for assessing site effects in the Bovec basin (NW
326 Slovenia) related to 1998 Mw5.6 and 2004 Mw5.2 earthquakes. *Engineering Geology*,
327 91(2–4), 178–193. <https://doi.org/10.1016/j.enggeo.2007.01.008>.
- 328 Gosar A, Rošer J, Motnikar BŠ, & Zupančič P (2010) Microtremor study of site effects and
329 soil-structure resonance in the city of Ljubljana (central Slovenia). *Bulletin of Earthquake*
330 *Engineering*, 8(3), 571–592. <https://doi.org/10.1007/s10518-009-9113-x>.
- 331 Hadiwidjojo PMM, Samodra H, & Amin TC (1998) *Geological Map of The Bali Sheet*.
- 332 Herak M (2008) ModelHVSR—A Matlab tool to model horizontal-to-vertical spectral ratio of
333 ambient noise. *Computers & Geosciences*, 34, 1514–1526.
334 <https://doi.org/10.1016/j.cageo.2007.07.009>.
- 335 Kanai K (1983) *Engineering Seismology*. University of Tokyo Press.
- 336 Konno K, & Ohmachi T (1998) Ground-motion characteristics estimated from spectral ratio
337 between horizontal and vertical components of microtremor. *Bulletin of the Seismological*
338 *Society of America*, 88(1), 228–241. <https://doi.org/10.1785/bssa0880010228>.
- 339 Kurniawan R, Eva MN, Marjiyono M, & Sismanto S (2017) Pemetaan daerah rawan resiko
340 gempa bumi menggunakan metode hvsr di kotamadya denpasar dan sekitarnya, bali.
341 *KURVATEK*, 2(1), 21–30.
- 342 Lantada N, Pujades LG, & Barbat AH (2009) Vulnerability index and capacity spectrum based
343 methods for urban seismic risk evaluation. A comparison. *Natural Hazards*, 51(3), 501–
344 524. <https://doi.org/10.1007/s11069-007-9212-4>.
- 345 Mucciarelli M, Herak M, & Cassidy J (2007) *Increasing Seismic Safety by Combining*

- 346 *Engineering Technologies and Seismological Data* (Vol. 148). Springer.
- 347 Murdiantoro RA, Sismanto S, & Marjiyono M (2016) Pemetaan Daerah Rawan Kerusakan
348 Akibat Gempabumi Di Kotamadya Denpasar dan Sekitarnya dengan Menggunakan
349 Analisis Mikrotremor, Studi Kasus : Gempabumi Seririt 14 Juli 1976. *Jurnal Fisika*
350 *Indonesia*, 20(2), 36. <https://doi.org/10.22146/jfi.28373>.
- 351 Nakamura Y (1989) A Method For Dynamic Characteristic Estimation Of Surface. *Quarterly*
352 *Reports Of The Railway Technical Research Institute*, 9.
- 353 Nakamura Y (1997) Seismic vulnerability indices for ground and structures using microtremor.
354 *World Congress on Railway Research*, 1–7.
- 355 Nakamura Y (2000) Clear identification of fundamental idea of Nakamura's technique and its
356 applications. *Proceedings of the 12th World Conference on ...*, Paper no. 2656.
357 http://www.sdr.co.jp/papers/n_tech_and_application.pdf.
- 358 Över S, Büyüksaraç A, Bektaş Ö, Filazi A (2011) Assessment of potential seismic hazard and
359 site effect in Antakya (Hatay Province), SE Turkey. *Environmental Earth Sciences*, 62(2),
360 313-326.
- 361 Prakosa PT, Ibad MI, Kafi MS, Burhanudin MA, & Rahmania A (2015) Earthquake
362 Microzonation and Strength Building Evaluation at Gelora Bung Tomo Stadium Surabaya
363 Using Micro-Tremor Method. *Proceedings of the 2014 International Conference on*
364 *Physics and Its Applications*, 1(Icopia 2014), 14–20. [https://doi.org/10.2991/icopia-](https://doi.org/10.2991/icopia-14.2015.3)
365 14.2015.3.
- 366 Pratama IPD, Priyanto DK, & Negara PKGA (2020) Ambient Seismic Noise Analysis of Nyepi
367 Celebration Day in Denpasar , Bali Using Horizontal-to-Vertical Spectral Ratio (HVSR).
368 *Jurnal Geofisik*, 18(01), 23–26.
- 369 Sato T, Nakamura Y, & Saita J (2008) the Change of the Dynamic Characteristics Using

- 370 Microtremor. *World Conference on Earthquake Engineering, October.*
- 371 Sungkono, Warnana DD, Triwulan, & Utama W (2011) Evaluation of Buildings Strength from
- 372 Microtremor Analyses. *International Journal of Civil & Environmental Engineering*
- 373 *IJCEE-IJENS, 11(5), 8.*
- 374 Tokimatsu K (1995) Geotechnical site characterization using surface waves. *1st Intl. Conf.*
- 375 *Earthquake Geotechnical Engineering, 1333–1368.*
- 376 Triwulan, Utama W, Warnana, DD, & Sungkono (2010) Vulnerability Index Estimation for
- 377 Building and. *International Seminar on Applied Technology, Science and Arts, 1–5.*
- 378 Wulandari A, Suharno S, Rustadi R, & Robiana R (2018) Pemetaan mikrozonasi daerah rawan
- 379 gempabumi menggunakan metode hvsr daerah painan sumatera barat. *Jurnal Geofisika*
- 380 *Eksplorasi, 4(1). <https://doi.org/10.23960/jge.v4i1>.*
- 381